Dicle University
Journal of Engineering

https://dergipark.org.tr/tr/pub/**dumf**
duje.dicle.edu.tr

Investigation of Diffusion Welding With SX Steel Itself Using Different Interlayer Materials

Jiyan Güney[1], Selçuk Keskin[2], Haluk Kejanlı[3]*

1 Dicle University, Mechanical Department, jiyanguney21@outlook.com, Orcid No: 0000-0003-0168-6983

2 Dicle Üniversitesi, Mechanical Department, mselcuk.keskin@dicle.edu.tr Orcid No: 0000-0001-6233-1807

3 Dicle University, Mechanical Department, kejanlih@dicle.edu.tr, Orcid No: 0000-0002-4987-6316

ARTICLE INFO	ABSTRACT
	SX steels, a type of stainless steel enriched with high silicon content, are frequently used in critical applications of the industry due to their resistance to many acids. Areas of use are acid tanks, acid coolers, acid pipe systems and acid radiators. Increasing areas of use have increased the need to combine with different materials. This study aimed to join the different layers by diffusion welding method using Cu, Ni, Al7072 and Al8079. The samples were combined by keeping them under 5 MPa pressure for 60 minutes at 1000°C in an argon gas environment. Phase changes occurring in the junction area due to the effect of different interlayers were tried to be determined by SEM-EDS and XRD analyses. The changing metallographic structure of the intermediate layers was examined using an optical microscope, and the microhardness change of the joining region was determined with the HV hardness measuring device. While alpha-ferrite structure was observed in the Cu interlayered connections in the samples, multiphase structures were observed in the Al7072 and SX-Al8079 interconnected samples, and the presence of intermetallic phases was detected in both the interface and diffusion zones in the Ni interlayered samples.

Introduction

Diffusion welding is a method of joining two solid surfaces. Metals with sanded and cleaned surfaces are combined by creating bonds at the atomic level using parameters such as temperature, pressure and time [1]. Babayev and his team determined that the optimal bonding temperature was 1200°C by producing Fe/Cu/C and Fe/Zn/C pieces through the diffusion method. They observed that the resulting structures consisted of pearlite and ferrite components. Significant precipitation of Cu at the grain boundaries of the Fe/C alloy was clearly seen through energy-dispersive spectroscopy analysis conducted on the component welded at 1050°C. The accumulation of Cu at the ferrite and grain boundaries reduced hardness. Hardness values were higher in the inner cylindrical section due to the presence of copper composition. Generally, a decrease in hardness was observed in regions close to the welding zone in the inner cylindrical section. The cause of this hardness decrease was the diffusion of copper towards the outer part [2]. Surface roughness plays a crucial role in influencing the diffusion behavior of atoms during the process of diffusion bonding. In the context of diffusion bonding between 304 stainless steel

and pure nickel, it is observed that steel atoms exhibit a higher level of activity, consequently leading to an enhanced diffusion phenomenon. Hence, it is imperative to adjust the surface roughness towards nickel to attain a more robust bond between steel and nickel materials. Additionally, with an increase in temperature, there is a corresponding increase in the number of atoms diffusing towards the opposite side, further influencing the bonding process [3]. SEM analyses conducted on microstructure samples' interfaces revealed a seamless bonding between the Ni interlayer and duplex stainless steel. This occurred simultaneously with the diffusion of Ni, causing a transformation in the original material's ferrite + austenitic grain structure into an austenitic structure within the diffusion zone. Subsequent microhardness analyses performed on the cross-section of microstructure samples exhibited lower hardness in the interlayer as anticipated, in comparison to both the base material and the diffusion zone [4]. Dissimilar welds lacking an interlayer displayed diminished strength, lower notch tensile strength, and reduced impact toughness when compared to their respective parent

materials. Post-weld heat treatment further exacerbated the reduction in toughness compared to the as-welded condition. Conversely, such trends were not evident in welds incorporating a nickel interlayer, suggesting that nickel served as an effective diffusion barrier even during post-weld heat treatment [5]. The present study illustrates that the inclusion of a Ni interlayer improves the viability of welding WC-12Co cermet to SC45 steel using friction stir lap welding. In shear lap tensile tests, the initiation of fracture occurs at the interface between steel and cermet and propagates within the cermet for joints without Ni. In contrast, for joints with Ni, fracture takes place within the base materials. The Ni layer plays a role in forming a solid solution that imparts the joint with a graded coefficient of thermal expansion [6]. The interdiffusion between Al and Fe atoms is exceptionally rapid, with the interdiffusion coefficient being 4 orders of magnitude higher compared to the scenario under thermal equilibrium [7]. A direct diffusion bonded joint of aluminium alloy 5A02 and stainless steel SUS304 has been formed without incorporating any interlayer material. The welding time significantly influences the tensile shear strength of the joint. When the welding time is set at 60 minutes, the strength of the joint reaches a maximum of 101.3 MPa. XRD analysis indicates the presence of intermetallic phases such as Al_5Fe_2 and $Al_{13}Fe_4$ formed during the reaction. Microstructure investigation reveals that the thickness of the reaction layer monotonously increases with the welding time [8]. The Energy Dispersive X-ray Spectroscopy (EDS) analysis of the joints reveals that the developed layers in zones A, B, and C, progressing from the Mg side towards the Al side, consist of $\gamma(Al_{12}Mg_{17})$, a combination of γ and $\beta(Al_3Mg_2)$, and a blend of γ and β with a relatively higher mass fraction of β, respectively [9]. The utilization of nano-layered interlayers within the Ti/Al system, specifically in the form of a foil with a composition closely approximating equiatomic ratio, has been confirmed to yield flawlessly bonded joints in vacuum diffusion welding. This is particularly evident at reduced welding pressures, showcasing the efficacy of such interlayers in facilitating the creation of defect-free joints in alloys based on γ-TiAl intermetallic compounds [10]. It is clearly seen that hardness values are relatively decreased at locations where the Al sublayer is present. Hardness in areas where the Al sublayer diffuses closely aligns with the hardness values of the base materials [11]. The initiation of Ni/Al/Ni joint formation commences with the interaction between liquid aluminium (Al) and solid nickel (Ni), giving rise to the formation of the Al_3Ni intermetallic phase. Subsequently, solid-state interdiffusion progresses, leading to the sequential development of various phases: Al_3Ni_2, stoichiometric AlNi, Ni-rich AlNi, and $AlNi_3$. During intermediate stages of annealing, it is possible for two to four phases to coexist simultaneously [12]. The composition of the interfacial layer determined by EDX analysis was found to be 53.6% Al, 42.9% Fe, and 3.5% Mg. When the travel

speed in the Al 5754/DP600 lap weld was increased to 45mm/min, another interfacial layer was observed, albeit with fewer observed cracks [13]. At the interface between the steel and Al 99.8 filler, two intermetallic phases, Fe_2Al_5 and $FeAl_3$, have been formed. The thickness of the intermetallic phase seam measures approximately 2.3μm, notably thinner than analogous intermetallic phase seams achieved through other joining processes within the same system. The Fe_2Al_5 phase is characterized by trapezoidal, nearly equiaxial single grains surrounded by aluminium-rich remnants of the steel grains. The growth direction of the Fe_2Al_5 crystals does not align with their longest crystal axis [14]. Cracking of an alloy during solidification is a significant defect in both welds and castings. In welding, it is commonly referred to as solidification cracking [15]. Solidification cracking is prominently observed in the central region of the interlayer due to increased thermal stresses and the presence of rich phases in the central area of the specimens. The density of intermetallic phases increases with rising temperature [16]. Closed-form equations are used to measure the susceptibility to cracking during the solidification process following welding. These equations provide results consistent with crack susceptibility tests of binary Al alloys and are considered a reliable reference in studies in this field [17]. Increasing temperature heals internal cracks. During the recovery process, the previous crack area fills with fine grains. Then, with the rise in temperature, the fine-grained area gradually disappears [18]. The bonding temperature significantly affects the welding performance of joints. At a low bonding temperature, specifically 925°C, inadequate bonds are formed due to the sluggish diffusion of constitutional elements provided by CoCrNi MEA, hindering the diffusion process. Successful diffusion-welded joints can be achieved by employing a bonding temperature of 1075°C with a 1-hour holding time and applying a compressive pressure of 5 MPa [19]. The DSC results reveal that the Al_2O_3-25 wt% YSZ composite exhibits a higher heat flow compared to both aluminium alloy and other ceramic compounds as the temperature increases to 300°C. Consequently, it is envisaged that, during friction welding, the Al_2O_3-25 wt% YSZ composite would have the capability to efficiently transmit heat at an accelerated rate, even under low welding speeds. This characteristic is expected to enhance the overall weldability of the material to aluminium alloy [20]. Increased temperatures led to an acceleration of the diffusion mechanism, resulting in a reduced diffusion period necessary to achieve comparable coalescence. However, relatively inadequate coalescence was observed when the process temperatures ranged between 550-575°C [21]. The deformation of surface asperities through plastic flow and creep, the diffusion of atoms to voids across grain boundaries, grain boundary migration, and the volume diffusion of atoms to voids can be delineated as a sequential series of metallurgical stages in the process of diffusion bonding. Particularly, when

working with Ni-Ti alloys, diffusion bonding can be successfully accomplished even when adherent surface oxides are present [22].

The reviewed literature suggests that understanding the effect of the mechanical properties of welded joints on welding performance in welding processes applied will have a significant impact on determining the quality of the process.

In this study, the joining of SX steel by diffusion welding using four different intermediate layers was investigated. In the study, data on microstructure, microhardness, EDS analysis, SEM images and heat maps are presented. This particular material represents the first documented example in the literature of diffusion welding applied using different interlayers.

It is thought that the determined results will be important in future research, studies and also in solving industrial problems on this subject.

2. Material and Method

2.1 Materials

In this study, commercially available SX steel was joined by diffusion welding using different intermediate layers. 7072 and 8079 series pure aluminium, pure nickel and pure copper were selected as a result of literature research as the most suitable interlayer materials for this purpose. The chemical compositions of these materials are detailed in Table 1. The diffusion bonding process is elucidated in Figure 1.
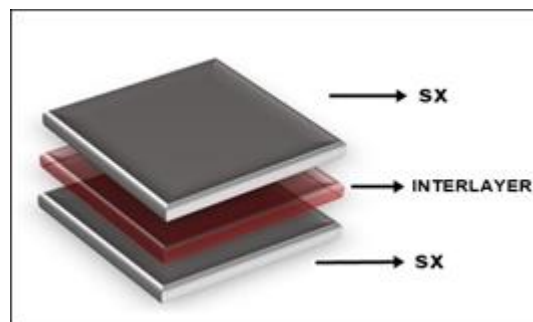
Figure 1. Diffusion welding process

Table 1. Chemical components of metals used in diffusion welding

Element	Fe	Al	C	Si	Mn	P	S	Cr	Ni	Mo	Cu
SX	55	-	≤0.025	5.0	0.5	≤0.045	≤0.030	17.5	19.5	0.4	2.0
Cu	99.5	-	-	-	-	-	-	-	-	-	-
Ni	98.5	-	-	-	-	-	-	-	-	-	-
Al7072	0.2	98.9	-	0.7	0.1	-	-	-	-	-	0.1
Al8079	0.7-1.3	98.65	-	0.05-0.3	-	-	-	-	-	-	0.05

2.2 Sample Preparation

Materials prepared in dimensions of 10x10x6 mm underwent a precise cutting process in a special liquid. This process was achieved using a cutting machine, ensuring uniformity in dimensions. Prior to the welding process, great care was taken in cleaning the surfaces of the metal elements. This was accomplished through a series of sanding stages using water-based sandpapers with grain sizes of 180, 240, 360, 400, 600, and 800. Surfaces were meticulously cleaned, preparing the metals for the next welding process. To facilitate the welding process, a specially designed clamp was used to compress the cleaned metal surfaces. This step is crucial to align and stabilize the metals during welding. Once securely clamped, the metals were placed in a

specialized diffusion furnace, where they were meticulously prepared for the welding process.

2.3 Diffusion Welding

Following the secure clamping of the samples, a critical stage commenced when they were precisely positioned inside a high-temperature furnace. As the welding process initiated, a pressure of 5 MPa was carefully applied, and argon gas with 99.9% purity penetrated the furnace at a controlled flow rate of 3 litters per minute. The welding process was conducted at a temperature of 1000°C for duration of 60 minutes. For proper reference, the exact parameters used in the diffusion welding process are provided in Table 2.

Table 2. Diffusion welding parameters

Parameter	Materials - Interlayer			
	SX-Cu	SX-Ni	SX-Al7072	SX-Al8079
Pressure (MPa)	5	5	5	5
Heat (°C)	1000	1000	1000	1000
Time (min)	60	60	60	60

2.4 Microstructure Studies

The samples, which underwent diffusion welding, were cut perpendicular to the interlayer. Subsequently, the surfaces were sequentially corrected with 400, 600, 800, 1000, 1200, and 2000 grit sandpapers. The roughness has a significant impact on the diffusion behaviour of atoms during the diffusion bonding of two different materials [3]. Following the sanding process, the surfaces were polished with 6μm diamond paste. To ensure cleanliness, the samples were then cleaned using alcohol in an ultrasonic vibration machine. Considering the high acid corrosion resistance of the SX steel used in the samples, two different etching agents were employed to enhance the visibility of the interlayer and diffusion zone microstructures. As the samples with copper and nickel interlayers were prepared for examination under an optical microscope, they were acidified using a solution containing 6 ml HF, 9 ml HNO_3, and 85 ml H_2O (referred to as King's Water). Conversely, samples with Al7072 and Al8079 interlayers were acidified using a solution containing 2.5 ml HNO_3 and 1.5 ml HCl. Samples requiring Keller

Solutions were treated with a mixture of 1 ml HF and 95 ml H_2O. Subsequently, the samples were thoroughly rinsed with water, cleaned with alcohol, and dried using hot dry air to prepare them for subsequent measurements.

2.5 Microhardness Studies

The evaluation of microhardness values of the samples was conducted using an AOB brand Vickers hardness measurement device. To obtain accurate measurements, a 50 g load was applied for 10 seconds. The calculation of averages involved obtaining three microhardness values at nine separate points, with approximately 13 μm intervals. Figure 2 illustrates the visual presentation of the sample on which microhardness measurements were performed.
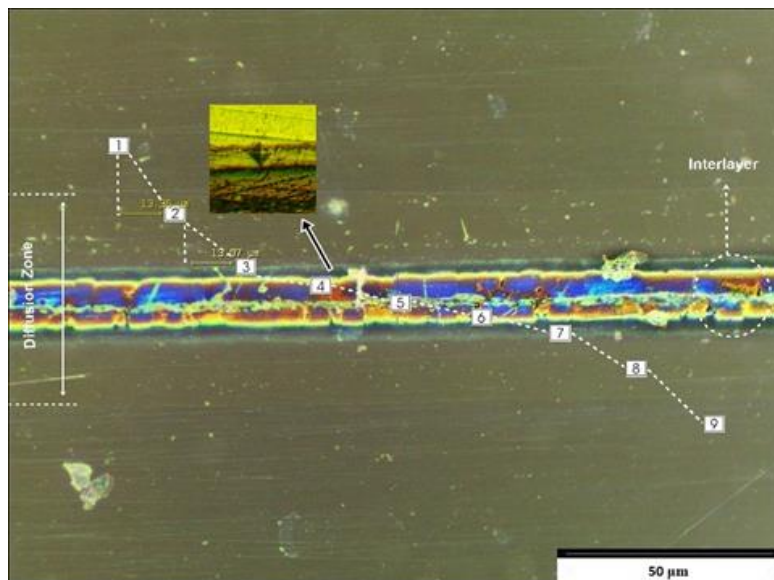
Figure 2. Location of microhardness points

3. FINDINGS AND DISCUSSION

3.1 Microstructure Results

SX steel has been welded with itself using diffusion welding, employing Cu, Ni, Al7072, and Al8079

interlayers. Diffusion welding processes were successfully carried out under a constant pressure of 5 MPa, at a fixed temperature of 1000°C, and for duration

of 60 minutes. In Figure 3, the formation of the α-ferrite structure is observed in the steel and copper junction [2]. In diffusion welding applications where nickel is used as a braze alloy, the material joined after welding does not lose its nickel's effective diffusion barrier properties even after undergoing heat treatment [5]. While diffusing SX steel with an Al pair, a significantly varied number of phase regions emerged in this bonding

process. The diffusion welding yielded excellent results in terms of microstructure. This is because the mutual diffusion between Al and Fe atoms is exceptionally rapid [7]. Mostly Al alloys and stainless steels are joined directly by diffusion welding [8]. Microscope images of the diffusion zones of the materials can be seen clearly in Figure 3, 4, 5 and 6.
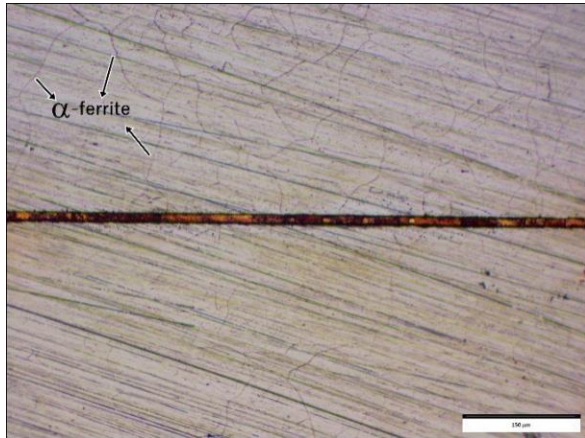
Figure 3. SX-Cu microstructure image
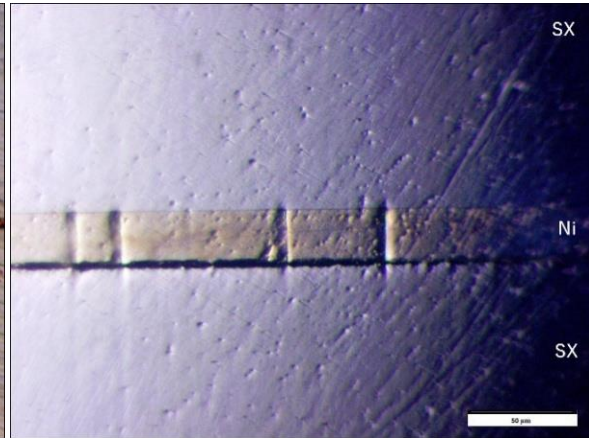
Figure 4. SX-Ni microstructure image
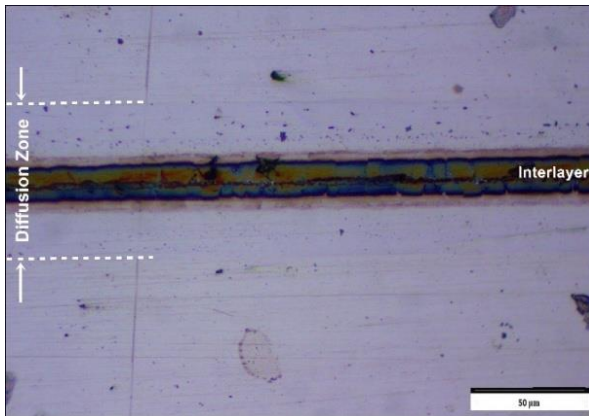
Figure 5. SX-Al7072 microstructure image
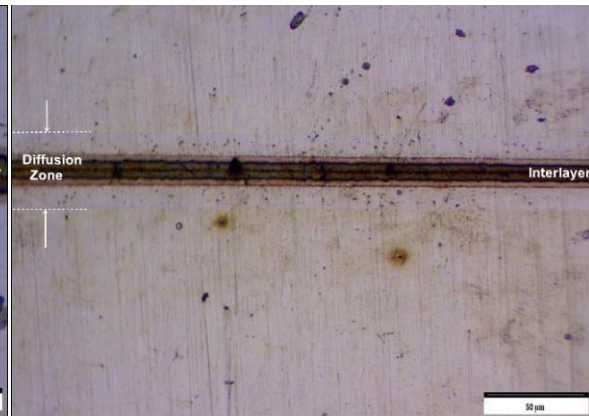
Figure 6. SX-Al8079 microstructure image

EDS Analysis results for all 4 diffusion sources are

shown with their detailed data in Figure 7 and 8.
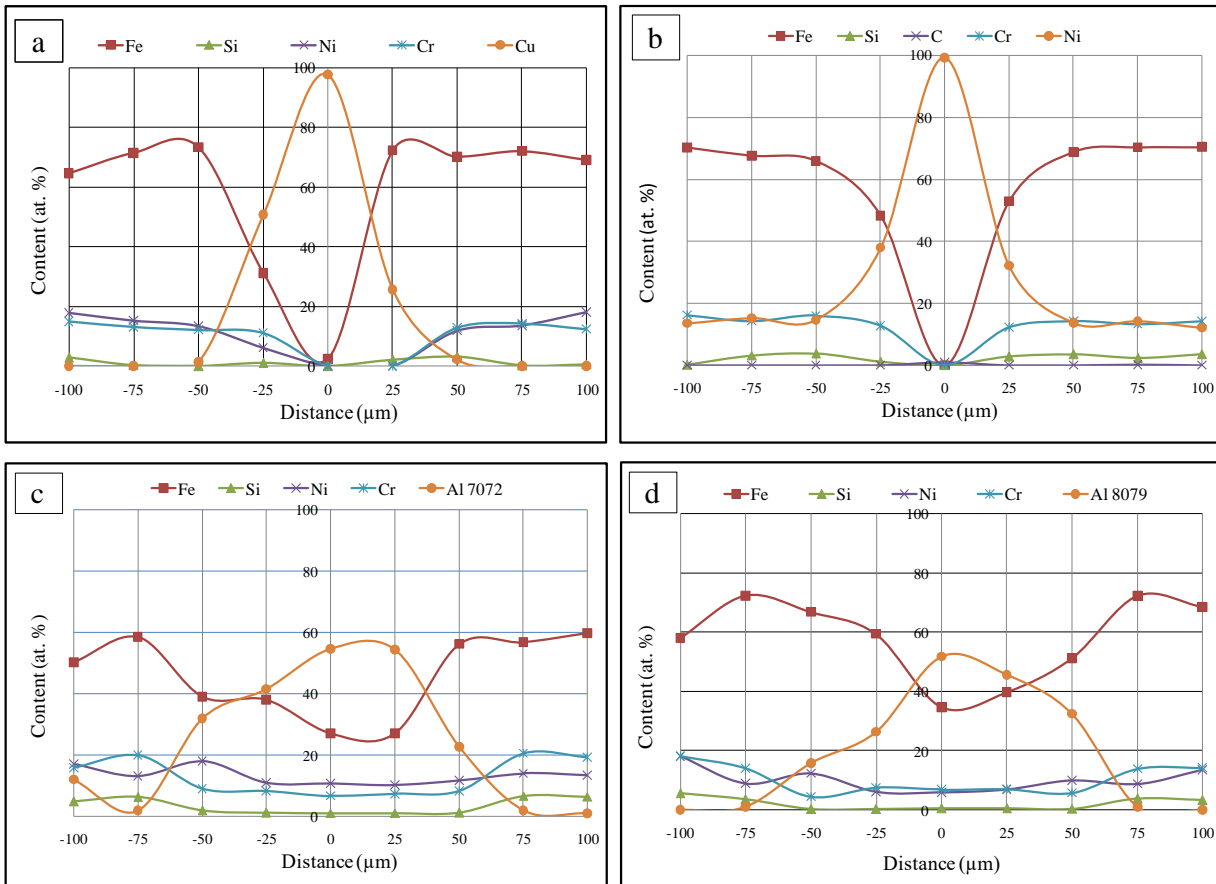
Figure 7. EDS analysis charts a) SX-Cu, b) SX-Ni, c) SX-Al7072, d) SX-Al8079
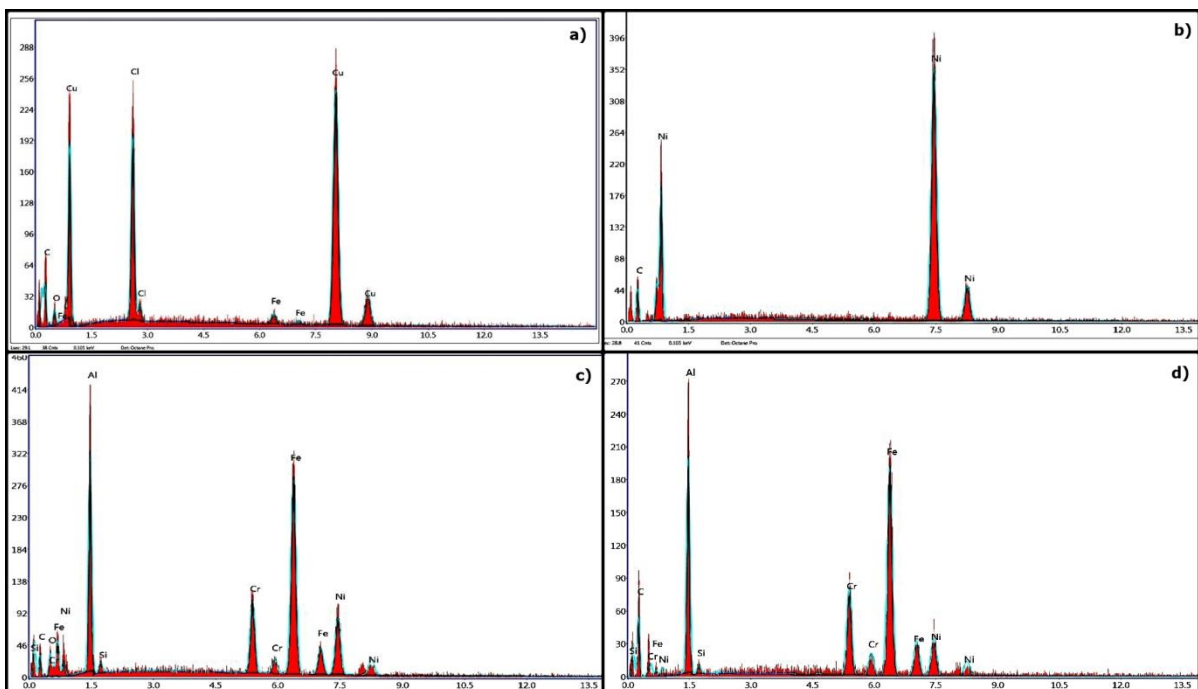
Figure 8. Detailed EDS analysis charts a) SX-Cu, b) SX-Ni, c) SX-Al7072, d) SX-Al8079

Looking at the 2nd and 4th analysis points of copper in Table 3, copper is located at the grain boundaries in the diffusion region of the steel. EDS analysis values at these points prove this [2]. In diffusion welding

applications where one of the joining materials is steel, the use of nickel as an interlayer enhances the feasibility of diffusion welding. As seen in Table 4, the nickel interlayer has exhibited diffusion and phase formation within the steel, spreading over long distances [6]. It is generally inevitable to see intermetallic phases in diffusion welding applications consisting of aluminium and steel [8]. EDS analysis values of the materials and the phase atoms formed are shown in Table 3, 4, 5 and 6.

Table 3. SX-Cu EDS analysis table

Analysis Points	C (at.%)	Fe (at.%)	Cr (at.%)	Cu (at.%)	Ni (at.%)	Si (at.%)	Detected Phases
1	-	73.33	13.19	-	13.48	-	Fe_6CrNi
2	-	31.49	10.48	50.7	6.33	0.96	$Fe_{16}Cr_6SiNi_3Cu_{23}$
3	-	2.28	-	97.72	-	-	$Cu_{113}Fe_3$
4	-	72.32	-	25.63	-	2.05	$Cu_{105}Fe_{337}Si_{19}$
5	-	71.21	12.82	-	12.84	3.13	$Fe_{11}Cr_2SiNi_2$

Table 4. SX-Ni EDS analysis table

Analysis Points	C (at.%)	Fe (at. %)	Cr (at. %)	Ni (at. %)	Si (at.%)	Detected Phases
1	-	65.79	15.96	14.58	3.67	$Fe_9Ni_2Cr_2Si$
2	-	48.2	12.73	37.95	1.12	$Fe_{22}Ni_{16}SiCr_6$
3	0.82	-	-	99.18	-	High nickel point
4	-	52.9	12.14	32.12	2.83	$Fe_9Ni_5SiCr_2$
5	-	68.74	14.22	13.56	3.48	$Ni_2Fe_{10}Cr_2Si$

Table 5. SX-Al7072 EDS analysis table

Analysis Points	Al7072 (at. %)	C (at. %)	Fe (at. %)	Cr (at. %)	Cu (at. %)	Ni (at. %)	Si (at. %)	Detected Phases
1	12.10	-	50.24	15.85	-	16.99	4.82	$Fe_5Cr_2SiNi_2Al_3$
2	1.99	-	58.45	19.98	-	13.22	6.36	$Fe_{14}Cr_5Si_3Ni_3Al$
3	32.00	-	38.95	9.03	-	18.05	1.97	$Fe_{10}Cr_2SiNi_4Al_{17}$
4	41.57	-	37.97	8.26	-	10.93	1.28	$Fe_{15}Cr_3SiNi_4Al_{34}$
5	54.55	-	26.98	6.71	-	10.67	1.08	$Fe_{13}Cr_3SiNi_5Al_{53}$
6	54.33	-	27	7.35	-	10.23	1.08	$Fe_{13}Cr_4 SiNi_5Al_{52}$
7	22.63	-	56.18	8.24	-	11.67	1.27	$Fe_{22}Cr_4SiNi_4Al_{19}$
8	1.87	-	56.8	20.56	-	14.05	6.72	$Fe_{15}Cr_6Si_3Ni_3Al$
9	0.96	-	59.78	19.31	-	13.45	6.49	$Fe_{30}Cr_{10}Si_6Ni_6Al$

Table 6. SX-Al8079 EDS analysis table

Analysis Points	Al8079 (at. %)	C (at.%)	Fe (at. %)	Cr (at. %)	Cu (at.%)	Ni (at. %)	Si (at. %)	Detected Phases
1	-	-	58.11	18.2	-	18.07	5.62	$Fe_5Cr_2SiNi_2$
2	1.02	-	72.31	14.07	-	8.94	3.66	$Fe_{34}Cr_7Si_3Ni_4Al$
3	15.84	-	66.88	4.52	-	12.42	0.34	$Fe_{99}Cr_7SiNi_{17}Al_{48}$
4	26.42	-	59.5	7.61	-	6.10	0.37	$Fe_{81}Cr_{11}SiNi_8Al_{74}$
5	51.8	-	34.74	6.93	-	5.95	0.59	$Fe_{30}Cr_6SiNi_5Al_{91}$
6	45.65	-	39.77	7.09	-	6.89	0.60	$Fe_{33}Cr_6SiNi_5Al_{79}$
7	32.5	-	51.22	5.78	-	10.04	0.45	$Fe_{57}Cr_7SiNi_{11}Al_{75}$
8	1.01	-	72.33	13.97	-	8.85	3.83	$Fe_{35}Cr_7Si_4Ni_4Al$
9	-	-	68.58	14.32	-	13.64	3.46	$Fe_{10}Cr_2SiNi_2$

It was observed that different phase regions formed between iron atoms and aluminium atoms [14].

Solidification cracking is a phenomenon seen in welding and casting applications [15]. Solidification cracking may arise as a result of elevated thermal stresses and the presence of enriched phases at the center of the interlayer. Consequently, the densities of intermetallic phases gradually decrease from the surface towards the center of the interlayer [16]. Closed-form equations, known as crack susceptibility index, have been derived to calculate the tendency for solidification cracking during diffusion bonding using $|dT/d(f_S)^{1/2}|$. The use of these equations is straightforward and provides insights into cracking during solidification after diffusion bonding [17]. SEM images detect internal cracks if they have formed [18]. The images of my materials under the SEM microscope are shown in Figure 9.
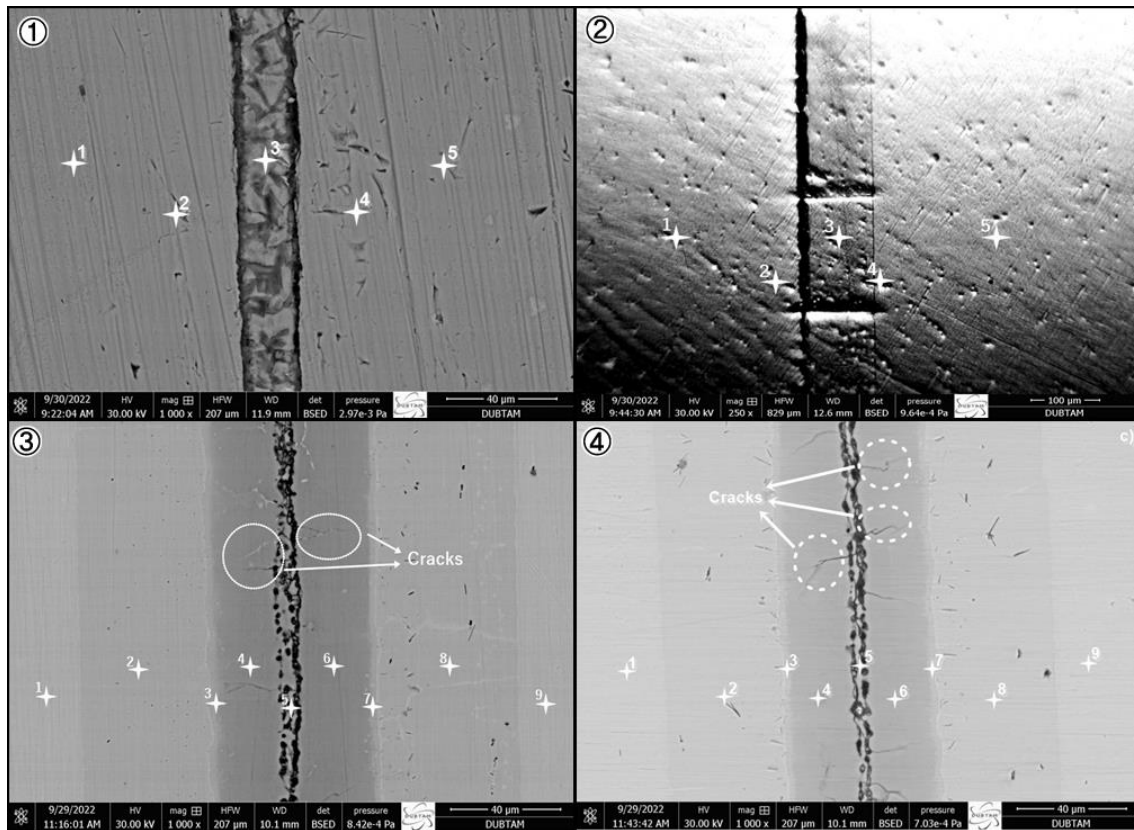
Figure 9. SEM images of materials 1) SX-Cu, 2) SX-Ni, 3) SX-Al7072, 4) SX-Al8079

3.2 Microhardness Results

In each of the four joints, Vickers hardness measurements were taken at nine different points. In the SX-Cu joint, as one moves from the steel region to the copper region, the hardness value decreases [2]. When the values for nickel are examined, sequential microhardness analyses performed on cross-sections of microstructure samples revealed lower hardness values in the interlayer compared to both the base material and the diffusion zone, as anticipated [4]. Depending on the Joined metal, in diffusion studies where the interlayer metal is aluminium, the hardness at points where aluminium sublayer diffuses is close to the hardness of the base material. This is valid in places where phase formation is not observed [11]. However, both Al7072 and Al8079 metals have formed phases to a good extent in the diffusion zone with SX steel. This has resulted in high hardness values at these points. These values are seen in Table 7 and Figure 10.

Table 7. Hardness measurement table of materials

Materials	Distance from the weld centre								
	-40	-30	-20	-10	0	+10	+20	+30	+40
SX-Cu	244.6	286.2	227.2	186.5	158.3	212.3	309.8	265.2	254.3
SX-Ni	271.0	265.2	218.5	126.7	116.6	103.0	212.7	353.3	255.7
SX-Al7072	243.9	277.1	841.0	508.8	459.9	809.9	780.4	246.6	238.9
SX-Al8079	236.5	324.7	593.4	713.5	371.4	689.1	677.4	254.2	234.1
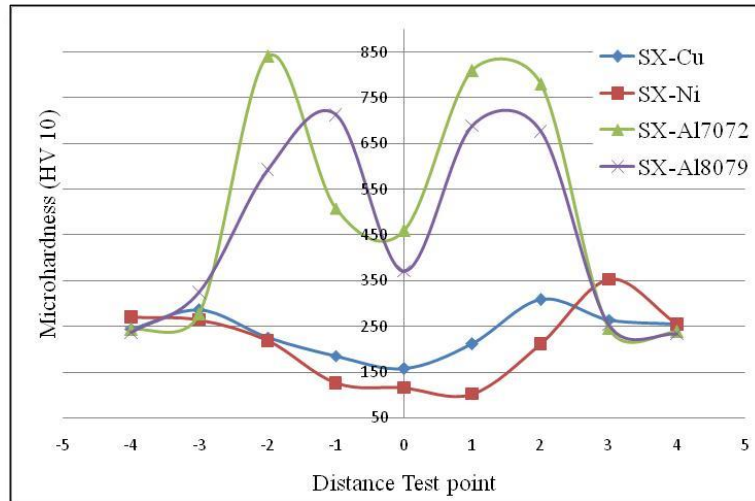
Figure 10. Hardness chart of materials

3.3 Heatmap Results

Heat map analysis was conducted for all four diffusion joints. Better heating data was observed in regions where diffusion occurred more prominently. During diffusion bonding, temperature plays a crucial role in interfacial diffusion; as the temperature increases, the number of atoms spreading to the opposite side and diffusion distances also increase [3, 21]. Bonding temperature significantly influences the welding performance of joints. At a low bonding temperature, poor bonds form due to the slow diffusion of elements, complicating the diffusion process. Successful diffusion-welded joints can be achieved by utilizing an optimal bonding temperature with a 1-hour holding time and applying a compressive pressure of 5MPa [19]. The heat distribution map of all four samples is clearly visible in Figure 11.
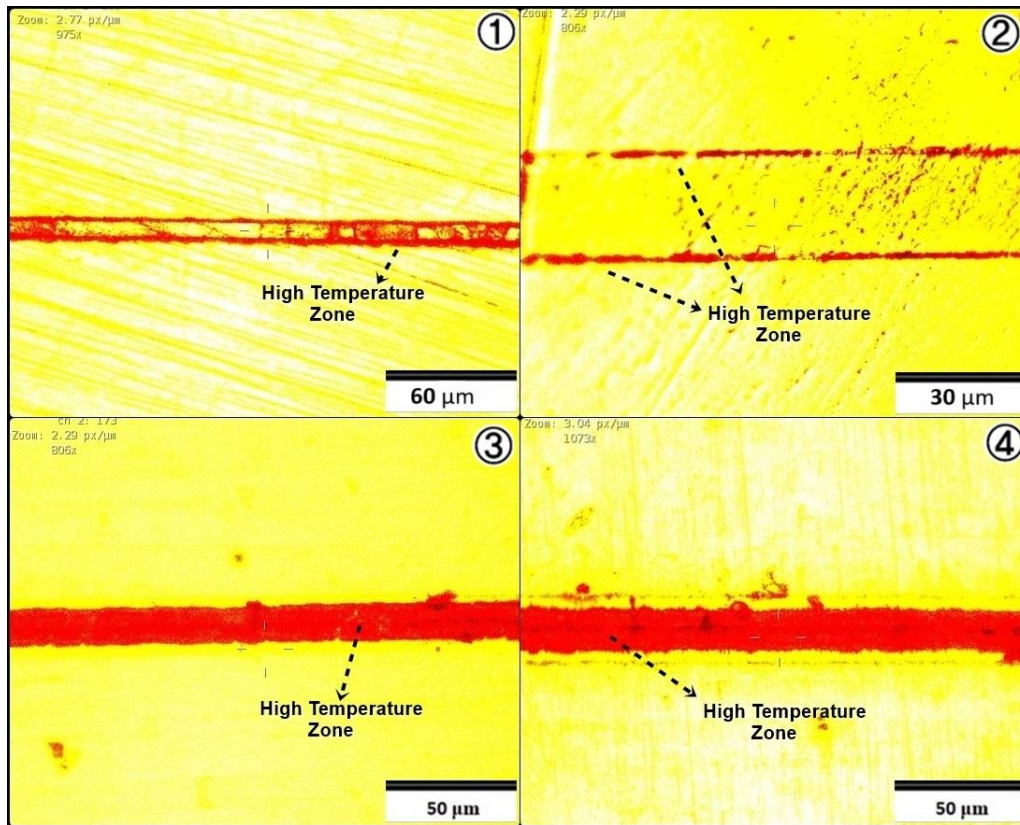
Figure 11. Heatmap of materials 1) SX-Cu, 2) SX-Ni, 3) SX-Al7072, 4) SX-Al8079

4. Conclusions

In this study, SX steel was successfully joined using the diffusion bonding method with copper, nickel,

- When the microstructures of the joints were examined, an alpha-ferrite structure was observed in the copper interlayered joints, while multiphase structures were observed in the SX-Al7072 and SX-Al8079 metal pairs, indicating extensive diffusion of the interlayers.
- EDS analysis results revealed high diffusion rates of intermetallic phases in both the interface and diffusion regions in SX-Cu and SX-Ni joints. On the other hand, high concentrations of iron diffusion were detected in both the interface and diffusion regions of SX-Al7072 and SX-Al8079 connections.
- SEM images showed microcracks on the aluminum (Al) surface in SX-Al7072 and SX-Al8079 joint pairs. This is attributed to the commonly encountered solidification temperature and the high density of intermetallic phases in the aluminum material.
- Hardness analysis conducted at nine points on all four materials indicated a decrease in
- hardness as one approached the diffusion regions for copper and nickel, while hardness values increased in the aluminum diffusion regions. This is believed to be a consequence of the higher ratio of

Al7072, and Al8079 interlayer materials. The obtained results are presented below:

intermetallic phases in SX-Al pairs.

- Heat map analysis of the materials revealed that diffusion occurred more extensively along the interface boundaries in SX-Cu and SX-Ni pairs. In SX-Al7072 and SX-Al8079 pairs, diffusion was observed from the interface center toward the boundary of the diffusion region. This was attributed to the higher diffusion rate at elevated temperatures, which made thermal heating more effective in Al pairs.
- In this study, a specialized welding technology was employed. Joining was accomplished in a diffusion bonding furnace within a laboratory environment with the aid of specific metallographic materials. While the equipment used in this process entails disadvantages in terms of cost compared to other welding techniques, the study's data on weld quality, microstructure, and microhardness elevate its significance above other welding methods.

This contribution to the literature provides valuable insights into its potential applications in the aerospace industry and the future of welding technology. In the future, researchers can combine these materials with different parameters and try to determine their

650

mechanical properties and contribute to the literature.

Ethics committee approval and conflict of interest

statement

"There is no need to obtain permission from the ethics

committee for the article prepared"

"There is no conflict of interest with any person / institution in the article prepared"

References

[1] Sathish, T., Kumar, S. D., Muthukumar, K., Karthick, S. Temperature distribution analysis on diffusion bonded joints of Ti-6Al-4V with AISI 4140 medium carbon steel. *Materials Today: Proceedings*, 21, 847-856, 2020.

[2] Babayev, Y., Kahraman, F., Karadeniz, S. A new approach on diffusion welding of Fe–Cu–C and Fe–Zn–C powder metal parts. *Materials and Manufacturing Processes,* 25(11), 1292-1296, 2010.

[3] Zhang, Y., Jiang, S. Atomistic investigation on diffusion welding between stainless steel and pure Ni based on molecular dynamics simulation. *Materials*, 11(10), 1957, 2018.

[4] Delice U, 1.4462 duplex stainless steel using nickel interlayer with diffusion welding with bonding, master's thesis, Nevşehir Hacı Bektaş Veli Üniversitesi / Fen Bilimleri Enstitüsü / Metalurji ve Malzeme Mühendisliği Ana Bilim Dalı, Nevşehir, 2021.

[5] Reddy, G. M., Ramana, P. V. Role of nickel as an interlayer in dissimilar metal friction welding of maraging steel to low alloy steel. *Journal of materials processing technology*, 212(1), 66-77, 2012.

[6] Avettand-Fènoël, M. N., Nagaoka, T., Fujii, H., Taillard, R. Effect of a Ni interlayer on microstructure and mechanical properties of WC-12Co cermet/SC45 steel friction stir welds. *Journal of Manufacturing Processes,* 40, 1-15, 2019.

[7] Wei, Y., Xiong, J., Li, J., Zhang, F., Liang, S. Microstructure and enhanced atomic diffusion of friction stir welding aluminium/steel joints. *Materials Science and Technology,* 33(10), 1208-1214, 2017.

[8] Shi, H., Qiao, S., Qiu, R., Zhang, X., Yu, H. Effect of welding time on the joining phenomena of diffusion welded joint between aluminum alloy and stainless steel. *Materials and Manufacturing Processes,* 27(12), 1366-1369, 2012.

[9] Azizi, A., Alimardan, H. Effect of welding temperature and duration on properties of 7075 Al to AZ31B Mg diffusion bonded joint. *Transactions of Nonferrous Metals Society of China,* 26(1), 85-92, 2016.

[10] Ustinov, A. I., Falchenko, Y. V., Ishchenko, A. Y., Kharchenko, G. K., Melnichenko, T. V., &Muraveynik, A. N. Diffusion welding of γ-TiAl based alloys through nano-layered foil of Ti/Al system. *Intermetallics*, 16(8), 1043-1045, 2008.

[11] Kejanlı, H., Avcı, M. T/M yöntemiyle üretilmiş Mg-Ti alaşımının difüzyon kaynağı ile birleştirilmesine aratabakanın etkisi. Dicle Üniversitesi Mühendislik Fakültesi Mühendislik Dergisi, 9(1), 279-289, 2018.

[12] Lopez, G. A., Sommadossi, S., Gust, W., Mittemeijer, E. J., Zieba, P. Phase characterization of diffusion soldered Ni/Al/Ni interconnections. *Interface science*, 10, 13-19, 2002.

[13] Haghshenas, M., Abdel-Gwad, A., Omran, A. M., Gökçe, B., Sahraeinejad, S., Gerlich, A. P. Friction stir weld assisted diffusion bonding of 5754 aluminum alloy to coated high strength steels. *Materials & Design,* 55, 442-449, 2014.

[14] Agudo, L., Eyidi, D., Schmaranzer, C. H., Arenholz, E., Jank, N., Bruckner, J., Pyzalla, A. R. Intermetallic Fe x Al y-phases in a steel/Al-alloy fusion weld. *Journal of materials science*, 42, 4205-4214, 2007.

[15] S. Kou, Welding Metallurgy, second ed., John Wiley and Sons, Hoboken, 2013, pp. 257–300.

[16] Ahmad, M., Akhter, J. I., Shahzad, M., Akhtar, M. Cracking during solidification of diffusion bonded Inconel 625 in the presence of Zircaloy-4 interlayer. *Journal of alloys and compounds*, 457(1-2), 131-134., 2008.

[17] Liu, J., Kou, S. Effect of diffusion on susceptibility to cracking during solidification. Acta Materialia, 100, 359-368, 2015.

[18] Han, J., Zhao, G., Cao, Q. Internal crack recovery of 20MnMo steel. Science in China Series E: *Technological Sciences*, 40, 164-169, 1997.

[19] Samiuddin, M., Li, J., Chandio, A. D., Muzamil, M., Siddiqui, S. U., Xiong, J. Diffusion welding of CoCrNi medium entropy alloy (MEA) and SUS 304 stainless steel at different bonding temperatures. *Welding in the World*, 65, 2193-2206, 2021.

[20] Uday, M. B., Fauzi, M. A., Zuhailawati, H., Ismail, A. B. Thermal analysis of friction welding process in relation to the welding of YSZ-alumina composite and 6061 aluminum alloy. *Applied Surface Science,* 258(20), 8264-8272, 2012.

[21] Taşkın, M., Çalıgülü, U. Modelling of microhardness values by means of artificial neural networks of Al/SiCp metal matrix composite material couples processed with diffusion method.

Mathematical and Computational Applications, 11(3), 163-172, 2006.

[22] Taskin, M., Dikbas, H., Caligulu, U. Artificial neural network (ann) approach to prediction of diffusion bonding behavior (shear strength) of ni-ti alloys manufactured by powder metalurgy method. *Mathematical and Computational Applications*, 13(3), 183-191, 2008.